Supporting Information

Pécsi et al. 10.1073/pnas.1013872108

SI Results and Discussion

The hDUT^{armless} Mutant Preserves Its Trimeric Structure. The C-terminal arm of dUTPase conferring the P-loop-like sequence leaves its protomer and spans another protomer to reach the active site of the third one (Fig. S2). We designed the armless mutation such that the sequence likely responsible for keeping the trimer together remains unaffected (1). We performed gel filtration chromatography with both the wild-type (WT) and the mutant (Fig. S3) and experimentally proved the intact nature of the expressed hDUT^{armless} protein (cf. ref. 2).

dUTPase Does Not Hydrolyze the dUDP.BeF$_x$ Complex. We investigated the mechanism of dUTP binding and hydrolysis by C-terminal motif V mutants, in which some or all of the secondary interactions between the γ-P and the enzyme are compromised. When using dUDP.BeF$_x$, however, we changed the properties of the γ-P and not of the protein. The bond between the β-P and the beryllium atom is thought to exhibit covalent features (3) while the fluoride is able to form H-bonds thus potentially mimicking a nucleoside triphosphate. Our efforts to crystallize the enzyme.dUDP.BeF$_x$ complex remained fruitless. However, we used fluorescence spectroscopy to gain insight into the binding mode of BeF$_x$. As shown in Fig. S7*A*, addition of Be^{2+} and F^- to the hDUT.dUDP complex results in a high quench of the Trp fluorescence ($F_{rel} = 0.35$) spectroscopically identical to that induced by dUPNPP. Such high fluorescence reduction is usually observed in hDUT.dUPNPP and hDUT.dUTP complexes (4, 5). Therefore, it is likely that BeF$_x$ binds to the γ-P site within the active site and induces similar conformation to that of the prehydrolysis analog dUPNPP.

The fluorescence measurements had already indicated that hydrolysis between the α- and β-phosphates probably does not occur as no fluorescence change could be observed within several hours of complex formation (the enzyme.dUMP complex is characterized by a fluorescence level close to the apo state). To confirm this result, we carried out additional experiments in single turnover conditions which also included an enzyme denaturation step so that even the enzyme-bound hydrolysis product would be freed into the solution. Fig. S7*B* displays the result of such an experiment using ion-exchange chromatography for the detection of the nucleoside released from the denatured enzyme. Compared to the control dUMP and dUDP chromatograms, no hydrolysis is apparent in the enzyme.dUDP.BeF$_x$ complex. We obtained similar results when samples were subjected to thin layer chromatography.

The enzyme.ADP.BeF$_x$ complex was shown to mimic the ATP-bound prehydrolysis conformations in myosin (6, 7) and other enzymes. It was also shown the ADP.BeF$_x$ analog is able to adopt the eclipsed conformation observed for dUPNPP in dUTPase (PDB ID: 2BEF) (8). We show that the complex is spectroscopically identical to the prehydrolysis complex formed with dUPNPP. It is therefore expected that the dUDP.BeF$_x$ analog is capable of forming adequate contacts with the P-loop-like motif V and transmitting conformational changes to the rest of the nucleotide analog. Surprisingly, however, it seems that the presence of γ-P in particular is necessary for hydrolysis to occur on the α-P suggesting that quantum chemical calculations are necessary to gain more insight into this phenomenon.

The Use of a P-Loop-Like Sequence to Promote Nucleotide Pyrophosphatase Activity and NDP/NTP Discrimination Is Unique in dUTPase. We carried out an extensive search in the literature to learn how other nucleotide pyrophosphatases achieve discrimination between nucleoside di- and triphophates. In nucleic acid polymerases, analyses of high resolution structures may simply explain that some structural elements essential for catalysis are missing when (d)NDP is bound into the active site [e.g., catalytic Mg^{2+} missing in Pol IV, (9)]. Other enzymes are suggested to work with large domain movements which promote an extensive interaction network between the γ-P and the enzyme necessary to achieve the hydrolysis-competent conformation [mRNA capping enzyme, ATP dependent DNA ligase (10, 11)]. In many cases, however, no mechanism of discrimination is proposed or inferred from the available data. The PDB database contains few structures with nucleotide pyrophosphatases liganded with (d)NDP. In the absence of structural data the function may help illuminate the mechanism of (d)NDP/(d)NTP discrimination. Most of these enzymes not only possess nucleotide pyrophosphatase activity but also possess phosphoryl transfer activity as well, thus coupling hydrolysis to a second reaction. In this case, the energy balance of (d)NTP hydrolysis may cover the cost of the secondary reaction while that of (d)NDP hydrolysis may not [$\Delta G^{\circ}_{ATP\rightarrow AMP} = -45.6$ kJ/mol vs. $\Delta G^{\circ}_{ADP\rightarrow AMP} = -32.6$ kJ/mol (12)].

Interestingly, we have not found any other example amongst the nucleotide pyrophosphatase enzymes which contains a P-loop-like sequence or P-loop to promote hydrolysis. It seems that dUTPase uniquely uses this widespread nucleotide binding motif for the hydrolysis of the α-β phosphate bond.

SI Methods

Circular Dichroism Intensity Titrations. CD spectra were recorded at 20 °C on a JASCO 720 spectropolarimeter using a 1 mm path length cuvette. 50 μM protein was titrated by stepwise addition of the nonhydrolysable substrate analog dUPNPP in a buffer containing 10 mM potassium-phosphate pH 7.5 and 1 mM $MgCl_2$. A spectrum between $\lambda = 250$–290 nm was recorded at each nucleotide concentration. Differential curves were obtained by subtracting the signal of dUPNPP alone from that of the corresponding complex. Differential ellipticity at $\lambda_{max} = 269$ nm was plotted against the dUPNPP concentration to obtain the binding curves. The following quadratic equation was fitted to the experimental curves:

$$y = s + A^*((c + x + K) - \sqrt{(c + x + K)^2 - 4^*c^*x})/2^*c$$

$s = y$ at $x = 0$; A = amplitude; c = protein concentration; $K = K_d$

Gelfiltration chromatography was carried out using a Superdex 200 10/30 GL column in an AKTA Purifier (GE Healthcare) chromatography system. Proteins were loaded in equal amounts and were subjected to isocratic elution in a buffer comprising 20 mM Hepes pH 7.5, 100 mM NaCl, 2 mM $MgCl_2$ and 1 mM DTT.

Steady-State Colorimetric dUTPase Assay. Protons released in the dUTPase reaction were detected by phenol red pH indicator in 1 mM Hepes pH 7.5 buffer also containing 100 mM KCl, 40 μM phenol red (Merck) and 5 mM $MgCl_2$. A Specord 200 (Analytic Jena, Germany) spectrophotometer and 10 mm path length thermostatted cuvettes were used at 20 °C. Absorbance was recorded at 559 nm. The Michaelis-Menten equation was fitted to the steady-state curves using Origin 7.5 (OriginLab Corp., Northampton, MA).

Ion-exchange chromatography was carried out using a BioScale Q2 (BioRad) column in an AKTA Purifier (GE Healthcare) chromatography system. 25 nmol dUMP/dUDP was loaded in a buffer containing 20 mM Hepes pH 7.5, 2 mM $MgCl_2$, 50 mM NaCl and 1 mM DTT followed by isocratic elution. The hDUT.dUDP.BeF_x complex was composed of 10 μM hDUT, 50 μM dUDP, 50 μM $BeCl_2$ and 2 mM NaF. The protein was removed from the solution before loading onto the column by heating followed by centrifugation.

Thin Layer Chromatography. 2.5 × 7.5 cm TLC Baker-flex plates coated with silica gel IB2-F (layer thickness, 0.2 mm) containing an UV254 fluorescence indicator were used (J. T. Baker, Germany, product number 4449-02). The following reaction solutions were prepaired: 85 μM WT dUTPase and $hDUT^{armless}$ mutant enzyme were mixed separately with 1 mM dUDP and incubated for 3 h at room temperature. To stop the reaction, 3 μL from the reaction mixture was incubated at 80 °C for 20 s after each hour. For control 1 mM dUMP was applied. 3 × 1 μL sample was loaded manually using a finely tapered micropipette tip, dried and run in a humidified glass beaker containing isopropanol/ammonium/water (v/v/v) 6:3:1 solution. When the solvent front has reached 1 cm from the top of the plate, the plates were dried completely with a hair dryer and exposed to UV light for evaluation.

1. Takacs E, Barabas O, Petoukhov MV, Svergun DI, Vertessy BG (2009) Molecular shape and prominent role of beta-strand swapping in organization of dUTPase oligomers. *FEBS Lett* 583:865–871.
2. Vertessy BG (1997) Flexible glycine rich motif of *Escherichia coli* deoxyuridine triphosphate nucleotidohydrolase is important for functional but not for structural integrity of the enzyme. *Proteins* 28:568–579.
3. Petsko GA (2000) Chemistry and biology. *Proc Natl Acad Sci USA* 97:538–540.
4. Toth J, Varga B, Kovacs M, Malnasi-Csizmadia A, Vertessy BG (2007) Kinetic mechanism of human dUTPase, an essential nucleotide pyrophosphatase enzyme. *J Biol Chem* 282:33572–33582.
5. Varga B, et al. (2007) Active site closure facilitates juxtaposition of reactant atoms for initiation of catalysis by human dUTPase. *FEBS Lett* 581:4783–4788.
6. Ponomarev MA, Timofeev VP, Levitsky DI (1995) The difference between ADP-beryllium fluoride and ADP-aluminum fluoride complexes of the spin-labeled myosin subfragment 1. *FEBS Lett* 371:261–263.
7. Fisher AJ, Smith CA, Thoden JB, Smith R, Sutoh K, Holden HM, Rayment I (1995) X-ray structures of the myosin motor domain of Dictyostelium discoideum complexed with MgADP.BeFx and MgADP.AlF4. *Biochemistry* 34:8960–8972.
8. Xu YW, Morera S, Janin J, Cherfils J (1997) AlF3 mimics the transition state of protein phosphorylation in the crystal structure of nucleoside diphosphate kinase and MgADP. *Proc Natl Acad Sci USA* 94:3579–3583.
9. Ling H, Boudsocq F, Woodgate R, Yang W (2001) Crystal structure of a Y-family DNA polymerase in action: a mechanism for error-prone and lesion-bypass replication. *Cell* 107:91–102.
10. Hakansson K, Doherty AJ, Shuman S, Wigley DB (1997) X-ray crystallography reveals a large conformational change during guanyl transfer by mRNA capping enzymes. *Cell* 89:545–553.
11. Sriskanda V, Shuman S (1998) Mutational analysis of Chlorella virus DNA ligase: catalytic roles of domain I and motif VI. *Nucleic Acids Res* 26:4618–4625.
12. Frey PA, Arabshahi A (1995) Standard free energy change for the hydrolysis of the alpha, beta-phosphoanhydride bridge in ATP. *Biochemistry* 34:11307–11310.

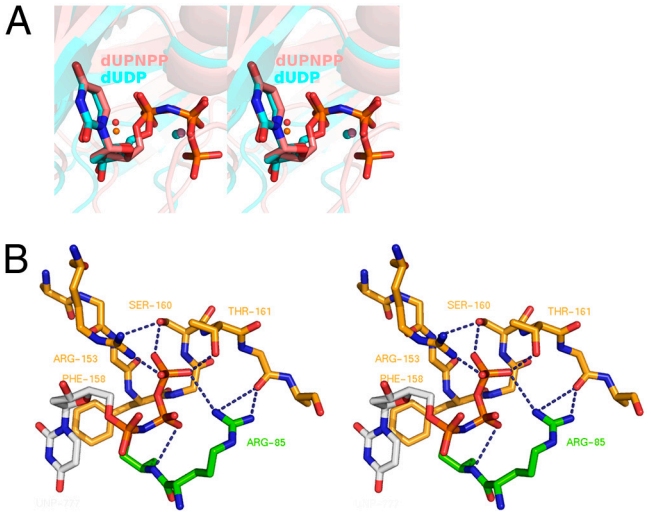

Fig. S1. Stereo representation of the structures displayed in (*A*), Fig. 1*B*; (*B*), Fig. 1*C*

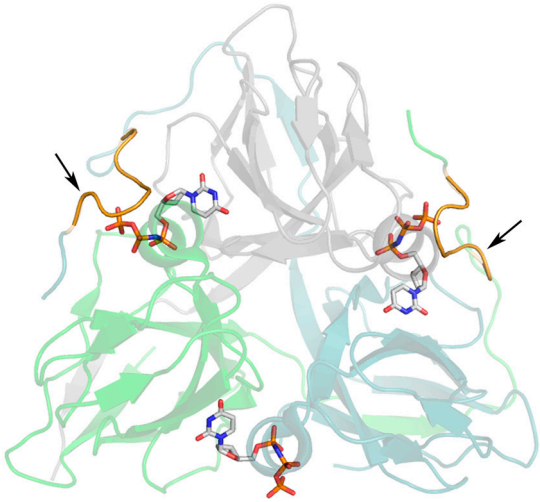

Fig. S2. The position of the P-loop-like motif in the trimeric structure of dUTPase. The structure of human dUTPase (PDB ID: 2HQU) is shown as a cartoon representation colored by subunits. The substrate analog dUPNPP is shown as a stick model (atomic coloring with gray carbons). The P-loop-like motives are highlighted in orange and pointed out by the arrows. Note that the C-terminal sequence of the gray subunit is missing from the refined structure and is therefore not shown. Also note that the loop isolates the bound nucleotide from the bulk solvent and surrounds the γ phosphate group.

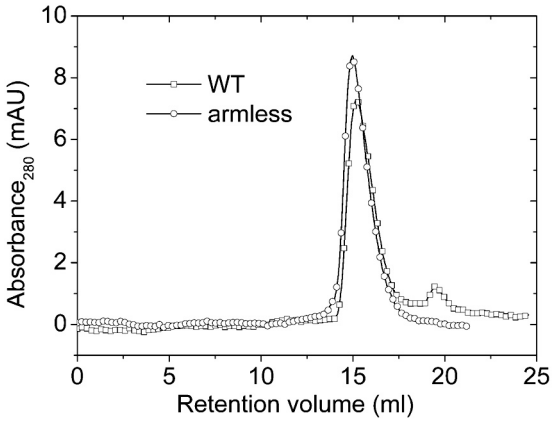

Fig. S3. Preservation of the trimeric quaternary structure in the hDUT^{armless} mutant demonstrated by gelfiltration. Purified WT (squares) and hDUT^{armless} (circles) proteins were subjected to gelfiltration chromatography in subsequent runs using the AKTA system equipped with a Superdex 200 10/300 column. The trimeric recombinant WT protein has a calculated molecular mass of 60 kDa. A trimeric hDUT^{armless} is calculated to be 55 kDa while its monomeric form would be 19 kDa- well separatable on a Superdex 200 column. A difference of 5 kDa, however, is not expected to be resolved. The retention volume was 15 mL for both proteins which indicated that deletion of the C terminus did not disturb the oligomerization of the hDUT^{armless} mutant. Consequently, the severe activity loss observed in this mutant is not due to an aberrant quaternary structure.

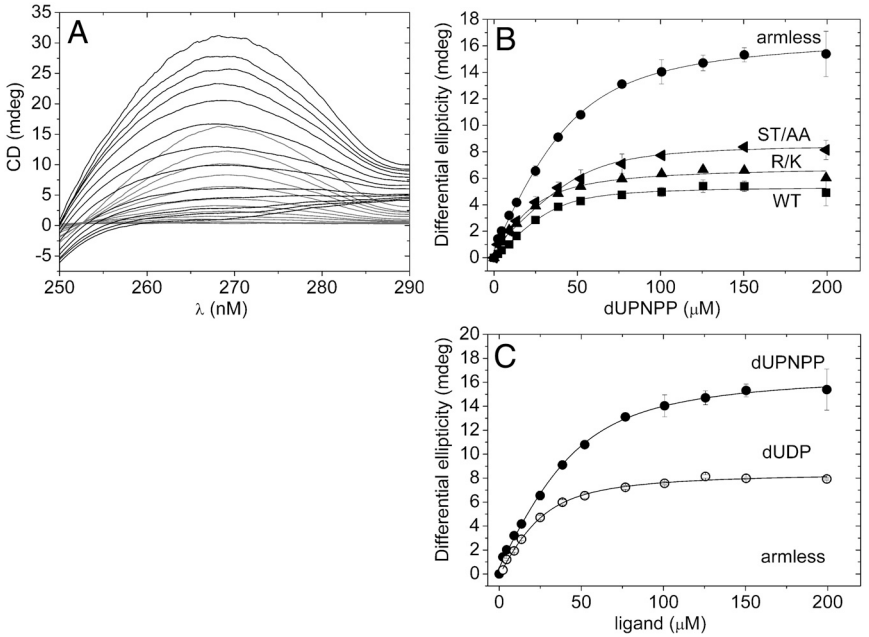

Fig. S4. Effect of mutations in the P-loop-like sequence on nucleotide binding as reported by CD. Fig. S4 shows CD equilibrium titrations of WT and mutant dUTPases by stepwise addition of the ligand (dUPNPP or dUDP). (*A*), CD spectra of 0–200 μM dUPNPP (gray lines) and its complex with 50 μM hDUT$^{R/K}$ (black lines). Such spectra were used to extract the maximal signal change at 269 nm in function of the ligand concentration to yield the binding curves shown in boxes (*B* and *C*). (*B*), Comparison of dUPNPP binding to the WT and mutant dUTPases. Solid lines represent hyperbolic fits to the data yielding the following K_d values: 3.4 ± 1.4 μM for WT (squares), 6.8 ± 2.9 μM for hDUT$^{ST/AA}$ (left-pointing triangles), 10 ± 4.1 μM for hDUT$^{R/K}$ (triangles), and 14 ± 0.43 μM for hDUT^{armless} (circles). (*C*) shows dUPNPP and dUDP binding to the hDUT^{armless} mutant. Hyperbolic fit to the data yielded a K_d of 9.5 ± 2.5 μM for dUDP (open circles) while the dUPNPP titration (solid circles) presented is identical with that seen in (*B*). Error bars represent SD for three or more independent measurements.

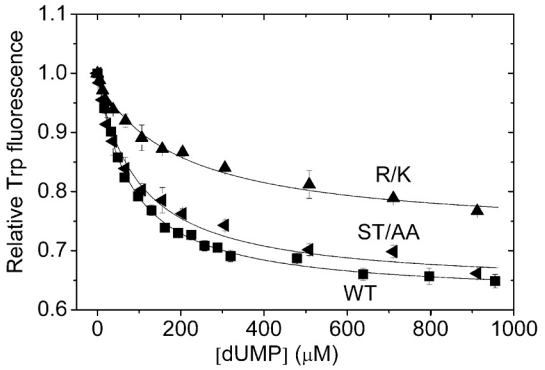

Fig. S5. Effect of mutations in the P-loop-like sequence on dUMP binding. Fluorescence intensity titration of the active site Trp is shown upon dUMP binding to WT (squares), hDUT$^{ST/AA}$ (left-pointing triangles), or hDUT$^{R/K}$ (triangles) dUTPase. Signal intensities are normalized to the nucleotide-free state. Smooth lines through the data are hyperbolic fits yielding K_d values of 78 ± 3.8 μM for the WT, 74 ± 5.6 μM for hDUT$^{ST/AA}$, and 96 ± 14 μM for hDUT$^{R/K}$. Error bars represent SD for three or more independent measurements. As the loop does not participate in dUMP binding, a significant change in the K_d or the maximal fluorescence quench of the protein.dUMP complex was not expected in the mutants.

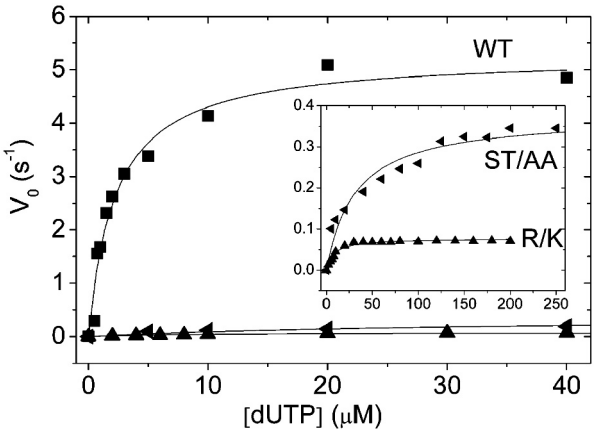

Fig. S6. Effect of mutations in the P-loop-like sequence on steady-state dUTPase activity. Michaelis-Menten curves for WT (squares), hDUT$^{R/K}$ (triangles), and hDUT$^{ST/AA}$ (left-pointing triangles) measured using the phenol red pH indicator assay. The inset shows the hDUT$^{R/K}$ and hDUT$^{ST/AA}$ curves enlarged. Fitting the Michaelis-Menten equation to the curves yielded the following V_{max} and K_M values: 5 s^{-1} and 2.3 μM for WT, 11.6 ± 1.74 μM for hDUT$^{ST/AA}$, and 6.1 ± 1.7 μM for hDUT$^{R/K}$. Similar curve for the hDUT^{armless} mutant could not be determined due to its largely diminished activity. Errors represent SD for $n = 3$.

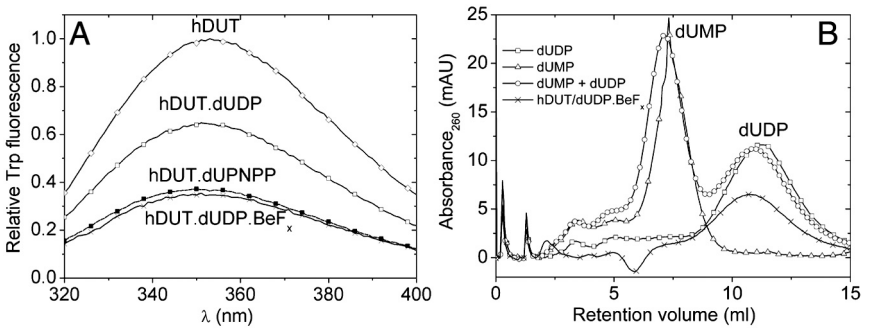

Fig. S7. Interaction of dUTPase with dUDP.BeF$_x$. (*A*), Trp fluorescence spectra of 10 μM WT ($F_{max} = 1$), its complex with 50 μM dUDP ($F_{max} = 0.64$), with 50 μM of the substrate analog dUPNPP ($F_{max} = 0.36$) and with 50 μM dUDP.BeF$_x$ ($F_{max} = 0.35$). The enzyme.dUDP.BeF$_x$ complex is composed of 10 μM WT, 50 μM dUDP, 50 μM $BeCl_2$, and 2 mM NaF. (*B*), Separation of dUDP and dUMP by ion-exchange chromatography on BioScale Q2 column to detect the end-product of dUTPase reaction with dUDP.BeF$_x$. dUMP (triangles) and dUDP (squares) were run separately or mixed together (circles) for reference. The enzyme.dUDP.BeF$_x$ complex (crosses) was incubated for several hours before chromatography. Only dUDP could be detected indicating that hydrolysis between the α-β phosphates did not occur.

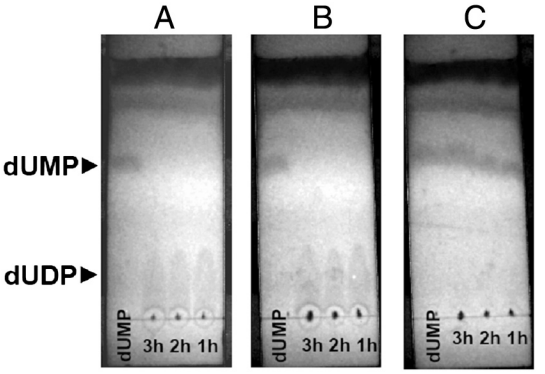

Fig. S8. dUDP is not hydrolyzed by either the WT or the C-terminally truncated enzyme. (*A*), 85 μM hDUT^{armless} was incubated with 1 mM dUDP for 1, 2, or 3 h at room temperature. The lack of any signal at the dUMP position indicates that hydrolysis did not occur. (*B*), 85 μM WT hDUT incubated with 1 mM dUDP. Hydrolysis is not detected. (*C*), Control dUTP hydrolysis by the WT hDUT shows the hydrolysed dUMP product. 1 mM dUMP was applied on each TLC plate for control.

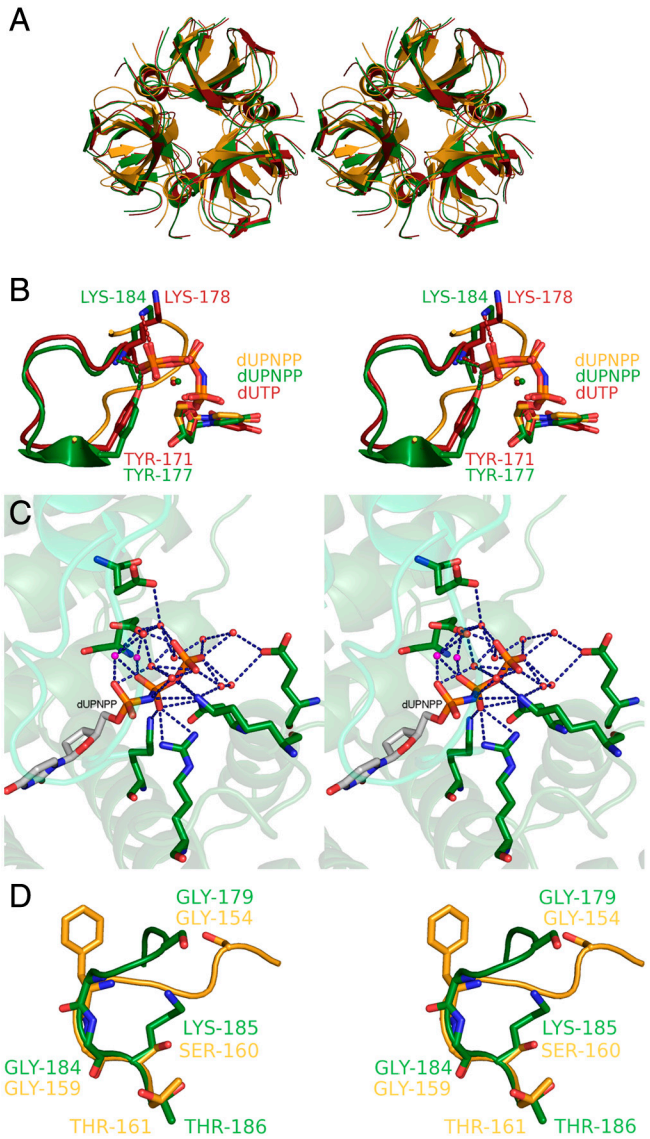

Fig. S9. Stereo representation of the structures displayed in (*A*), Fig. 4*A*; (*B*), Fig. 4*B*; (*C*), Fig. 4*C*; and (*D*), Fig. 4*E*